Journal of Glaciology

IGS

Article

Cite this article: Sundriyal S, Shukla T, Kang S, Zhang Y, Dobhal DP, Singh R (2024). Controls of lithology and climate over chemical weathering trends: new insights from the precipitation-dominated Dokriani glacier, central Himalaya, India. *Journal of Glaciology* 1–13. https://doi.org/10.1017/jog.2023.108

Received: 12 September 2023
Revised: 12 November 2023
Accepted: 19 December 2023

Keywords:
Chemical weathering; glaciers; Himalaya; ion stoichiometry; sulfide oxidation

Corresponding author:
Tanuj Shukla;
Email: tanuj.shukla@nieer.ac.cn

cambridge.org/jog

Controls of lithology and climate over chemical weathering trends: new insights from the precipitation-dominated Dokriani glacier, central Himalaya, India

Shipika Sundriyal[1], Tanuj Shukla[1], Shichang Kang[1,2], Yulan Zhang[1], Dwarika Prasad Dobhal[3] and Rajesh Singh[4]

[1]State Key Laboratory of Cryospheric Science, Northwest Institute of Eco-Environment and Resources, Chinese Academy of Sciences (CAS), Lanzhou 730000, China; [2]University of Chinese Academy of Sciences, Beijing 100049, China; [3]Wadia Institute of Himalayan Geology, Dehradun 248001, India and [4]Environmental Hydrology Division, National Institute of Hydrology, Roorkee 247667, India

Abstract

The chemical composition of meltwater-draining Himalayan glacierized basins reflects the dominance of carbonic acid in weathering of silicate and carbonate minerals, yet the role of sulfuric acid-mediated reactions in the mineral weathering and ionic release is still unclear. Here, we present a long-term study (1992–2018) of chemical weathering characteristics of a precipitation-dominated glacierized basin (Dokriani glacier) of central Himalaya. By using new and reprocessed datasets of major ions from the glacial/subglacial zones of the glacier, we suggest that two-thirds of the dissolved load of the meltwater derives from sulfuric acid-mediated weathering of minerals and rocks. We observed a clear control of carbonic acid-mediated reactions in the early ablation periods, while sulfuric acid-mediated reactions dominate in peak and late ablation periods. The slopes and intercepts in best-fit regressions of [$^{*}Ca^{2+} + {}^{*}Mg^{2+}$ vs $^{*}SO_4^{2-}$ and HCO_3^-] and [HCO_3^- vs $^{*}SO_4^{2-}$] in meltwater were following the stoichiometric parameters of sulfide oxidation coupled to carbonate dissolution reactions. The glaciers of the central and western Himalaya are in good agreement with the present estimates. We contend that the bedrock lithology has limited or second-order effects over the ionic release from Himalayan glaciers and surmise that these patterns are broadly applicable to the other orogenic systems of the world.

1. Introduction

Earth's elemental cycles are controlled through weathering process operating at subglacial and proglacial environments (Hodson and others, 2000; Wadham and others, 2010a, 2010b; Yde and others, 2014). However, this control is governed through variations in lithology i.e. nature/type of water-rock interactions and its rate in subglacial and proglacial environments along climate which influence these geochemical reactions throughout the ablation periods.

Glaciers (including ice sheets) that are not only known as an archive of snow and ice but also for processing the nutrients (Raiswell, 1984; Tranter and others, 1993; Anderson and others, 1997, 2000; Hasnain and Thayyen, 1999) and contaminants (Nijampurkar and others, 1993; Guzzella and others, 2016; Stachnik and others, 2016; Sundriyal and others, 2020) that deposits over the glacial surface and ultimately releases to downstream ecosystems (Tranter and others, 1993; Sharp and others, 1995; Wadham and others, 1998; Hodson and others, 2000; Cooper and others, 2002; Ferrario and others, 2017). As soon as the glacier melts, the lithological controls start to play its role. The coupling between geochemical reactions start at the glacial surface and become more intense as it travels through subglacial zones before its final evacuation through glacial termini (Tranter and others, 2002; Wadham and others, 2004, 2007). The meltwater chemistries sustained through these geochemical reactions and subsequent ionic release have already shown the dominance of carbonate weathering over silicate weathering at Himalayan glacierized basins (Hasnain and Thayyen, 1999; Singh and Hasnain, 2002; Shukla and others, 2018, 2020; Singh and others, 2020), while the importance of sulfuric acid-mediated weathering of carbonates has not given much attention at the Himalaya much likely due to their low abundance in underlying bedrocks. There is worldwide growing evidence that even with a low abundance of sulfide and carbonate minerals in the catchment can produce much variability in the ionic release due to their faster dissolution rates than silicate minerals (Williamson and Rimstidt, 1994; White and others, 1999; White and Brantley, 2003). Also, the oxidation of sulfides prominently influences the global budgets of redox-sensitive elements including sulfur, iron and oxygen (Berner and Canfield, 1989; Torres and others, 2014). Thus, considering the chemical erosion rates of glaciated terrains are predicted to be usually near to or greater than the continental average (likely due to high specific runoff with high concentrations of freshly comminuted rock flour, typically of silt-sized fractions coated with microparticles or surface precipitates), the glacial chemistries sustained through subglacial weathering should enrich the solute fluxes of the Himalayan glaciers. However, the operational effectiveness of the subglacial weathering is still a contention of

research where few studies suggest the solute enhancement due to the subglacial process (Anderson and others, 2000; Egli and others, 2021) whereas a few do not support this contention (Wadham and others, 2001). Therefore, when evaluating solute flux transport from the Himalayan glacierized basins, it is essential to distinguish between the dominance of carbonic vs sulfuric acid-mediated reactions in the ionic release mechanism. Failure to make this distinction led to much confusion and creates systematic biases in future ionic flux transport and their attendant effects on climate change.

Since Himalayan glaciers are valley-type systems, where the geochemical reactions have an additional control i.e. climate which influence the bulk meltwater production and seasonal evolution of the subglacial drainage system significantly (Anderson and others, 1997, 2000; Hasnain and Thayyen, 1999; West and others, 2002). Recent studies have highlighted the variability in seasonal meltwater chemistries of the Himalayan glacial basins; yet, rarely any study has examined the prominent role of different acid types in Himalayan glacierized catchments at different ablation periods, despite their proven influence over organic matter cycling, precipitation/snowpack chemistry and chemical weathering reactions (Singh and Hasnain, 2002; Mitchell and Brown, 2008; Wadham and others, 2010a; 2010b). Also, it is still unclear about the mechanism and favorable environment at which sulfide oxidation proceeds (Wadham and others, 2007; Shukla and others, 2023). Therefore, it seems timely to explain how the chemical-weathering reactions in different ablation periods affect the solutions that give rise to meltwater chemistry which is more variable than previously explained. A broad overview of the chemical weathering characteristics at Dokriani glacier basin has been presented by Hasnain and Thayyen, (1999), where a distinct correlation of climate over the state of ionic fluxes were explained. In another study, Tiwari and others (2018) has presented the state of ions at the glacial basin, yet the detailed controls over ionic release from the basin are not yet fully understood. Here in present study, we collected meltwater samples for the years 2015–2018 and reassessed the dataset from previous studies (Hasnain and Thayyen, 1996, 1999; Tiwari and others, 2018) from the glacial basin to explain the long-term (1992–2018) ionic stoichiometry, influence of climate, lithology over chemical weathering trends in the basin. The main objectives of the study are as follows: (a) Characterize distinct ion stoichiometry of glacial meltwater caused by long-residence times and mixing process which skew the bulk chemistry towards diluted signals; (b) study the seasonal evolution of ions i.e. ionic release in early, peak and late ablation periods; (c) study the impact of different acids i.e. sulfuric acid or carbonic acid in an ionic release from Himalayan glacierized basins; and, (d) finally estimate the origin and control of ion release from central and western Himalayan glacierized basins.

2. Study area

2.1 Physiography

The studied glacier is situated in the Dingad subbasin of the Bhagirathi River basin originating from the Gangotri Glacier, Uttarakhand India. Dokriani is the main trunk glacier of the Dingad basin located at 30°48′–30°53′ N to 78°39′–78°51′ E and comprising an area of 77 km^2 (Fig. 1). The glacier is formed by the two cirques i.e. Draupadi ka Danda and Jaonli peaks at 5600 and 6632 m a.s.l. respectively and extends between elevations of 3965–6200 m a.s.l. in N to E direction. Having a length of ∼5.4 km, glacier covers an area ∼6.6 km^2 with 2.5 km of glacier width. The maximum width of the glacier is 1.7 km at the Equilibrium line Altitude (ELA) (Shukla and others, 2018). The ablation area is 3 km long spanning nearly 2.3 km^2, and nearly 10% is covered with debris (Pratap and others, 2015). The glacier drainage system regulates the supraglacial, englacial and subglacial channel systems. The supraglacial streams draining from Moulin's and the basal melt flow through the subglacial system. The discharge station of the Dingad basin is situated at Dingad stream (3820 m.a.s.l.) which is 1.25 km downstream of the snout of the Dokriani Glacier. The other salient features of the study area are presented in supplementary table S1.

2.2 Geology

The major rock type of the Dingad basin comprise metamorphic and granitic rocks. The basin falls under the zones of two major thrust systems i.e. the Munsiari Thrust (MCT-1) in the south and Trans Himadri Fault (THF) in the North (Fig. 1; Heim and Gansser, 1939; Valdiya, 1998). The major lithology of the glacierized part of Dokriani glacier valley consists of metamorphosed banded calc-silicate gneiss and calc-schist rocks interbedded with subordinate biotite-psammitic gneiss and granite pegmatite apatite veins of Pinadari Formation, Vaikrita group. The extent of quartzite rocks of Pandukeshwar Formation could be seen in the upper part of the glacier basin while the lowermost part of the valley lies in streaky and banded psammitic gneisses-garnet- kyanite rich muscovite biotite rocks of Joshimath Formation. The rest of the valley comprises mylonitized bodies of granodiorite interbedded with chlorite sericite schist and graphite schist of the Myunsiari Formation (Heim and Gansser, 1939; Valdiya, 1999). The average stoichiometry of the bed load mineral phase is presented in supplementary table S2.

2.3 Climate

The study area is characterized as humid during summer and dry cold in winter (Dobhal and others, 2008; Pratap and others, 2015). A manual meteorological observatory and automatic weather station installed at the (3760 m a.s.l.) base camp of Dokriani Glacier suggests nearly 120–140 cm of precipitation falls as rainfall and 200–400 cm as snowfall. Indian Summer Monsoon (ISM) is the major source of precipitation as rainfall while westerlies during winter months are responsible for snowfall in the glacier region. The summer precipitation as rainfall occurring during summer seasons constitutes up to 80% of seasonal precipitation with a peak around August month. The mean temperature variation in the valley is 17°C (June–August) to −10°C (December–February).

2.4 Glacial ablation trends

The glacier-wide mass balance of study from a recent study suggests an overall negative mass balance (−9.64 ± 2.32 m w.e.) for the last four decades (Azam and Srivastava, 2020). The catchment-wide runoff of Dokriani Glacier was 1.56 ± 0.10 $m^3 s^{-1}$ over the period of 1979–2018, where the average contribution is 44 ± 2% from rainfall followed by 34 ± 1% from snowmelt and 22 ± 2% from ice melt to total catchment runoff. Maximum snowmelt (1.94 ± 0.09 $m^3 s^{-1}$) occurs in July while maximum ice melt occurs in August (1.55 ± 0.18 $m^3 s^{-1}$, ∼37% of total ice melt) due to the least available snow cover.

3. Methodology

3.1 Field methods

Field investigations in the Dokriani glacier basin are carried out from October 2015 to 2018. Majorly the sampling period

https://doi.org/10.1017/jog.2023.108 Published online by Cambridge University Press

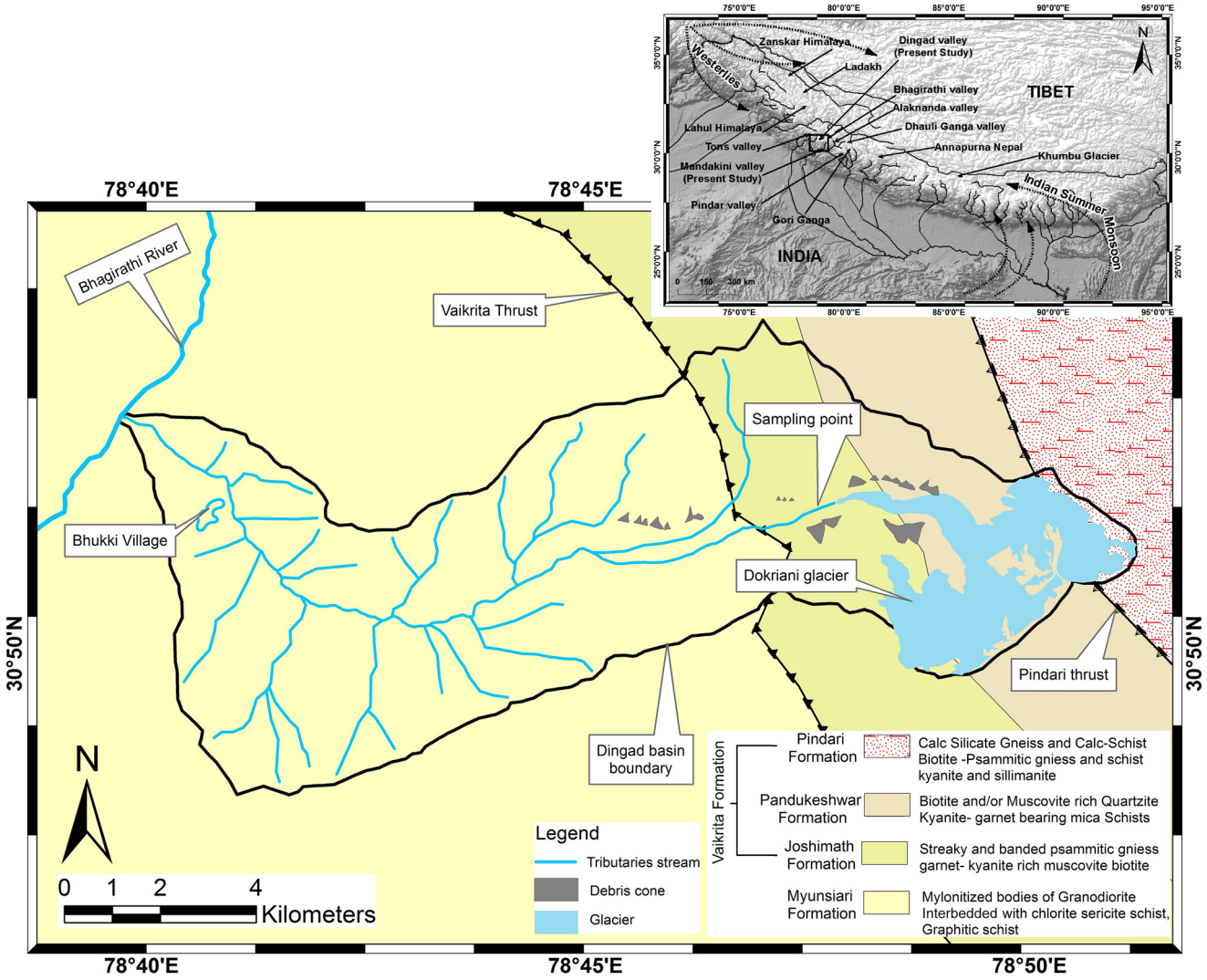

Figure 1. Geological and location map of the Dokriani glacier basin. Black square marked in the inset figure suggests the location of the study area in the Himalaya. The geological map setting of the study area was modified after Valdiya (1998).

is divided into early ablation, peak ablation and post-ablation periods, characterized by May–June, July–August and September–October months respectively. The meltwater samples have been collected from the Dingad stream, ~1.25 km downstream of the glacier snout (Figs 2a–c). The meltwater samples were collected in a precleaned 250 mL high-density polyethylene (HDPE) bottle and immediately filtered through a 0.22 µm Millipore polyethersulfone (PES) membrane using a Nalgene™ filtration tower and a handheld vacuum pump. Detailed sampling characteristics are presented in supplementary tables S3 and S4.

Measurements of physical parameters i.e. pH, electrical conductivity and water temperature, were performed in situ by using a multiparameter kit. The measurement precision of the instrument was as follows: pH ± 0.01 (SD 0.01); EC ± 1 µS cm^{-1}; water temperature ± 0.5°C. It measures pH up to 14 with a precision of ± 0.01 (SD 0.01). Before analysis, the pH and electrical conductivity probe were calibrated through standard solutions. Discharge measurement was done at the hydro-meteorological station by using surface velocity and water level measurements through the float flow method. The mean velocity, surface velocity and discharge are calculated by the area velocity method. For details of discharge estimations please refer to Kumar and others (2014).

3.2 Laboratory methods

3.2.1 Major ion and alkalinity measurements

Major cations (Ca^{2+}, Mg^{2+}, K^{+}, and Na^{+}) and anions (Cl^{-}, SO_4^{2-}, NO_3^{-}) were analyzed using a Metrohm® Ion Chromatograph system. Approximately 150 mL of the undiluted sample was injected on an anion column (Metrosep A SUP 5 250/4 mm with suppressor) in 50 mM L^{-1} Na_2CO_3 and 1.0 mM L^{-1} $NaHCO_3$ eluents, and in 1.7 mM L^{-1} dipiclonic acid with 1 mM L^{-1} HNO_3 on a cation column (Metrosep C 6 250/4 mm cation column). One blank (Milli-Q water) and one standard were injected after every 5 measured samples to check the accuracy and precision. The concentrations of ions in the sample were calculated based on a 5-point standard calibration curve. Analytical precision was within 5% for all the analytes (anions and cations) and accuracy was within 5%.

The total alkalinity (TA) was measured on a Metrohm® Potentiometric Auto Titrator (Model Number 888) by using 0.02 N H_2SO_4 as a titrant. The alkalinity of the solution has been classified as M alkalinity (pH indicator methylorange, endpoint 4.2 to 4.5) and P alkalinity (pH indicator phenolphthalein, endpoint 8.2–8.3). The overall titration accuracy was within 2.0%, and precision was within 1.5%. To maintain the precision of the samples and avoid the error in the data we performed repeat measurements of random samples. Results are shown in supplementary table S5.

https://doi.org/10.1017/jog.2023.108 Published online by Cambridge University Press

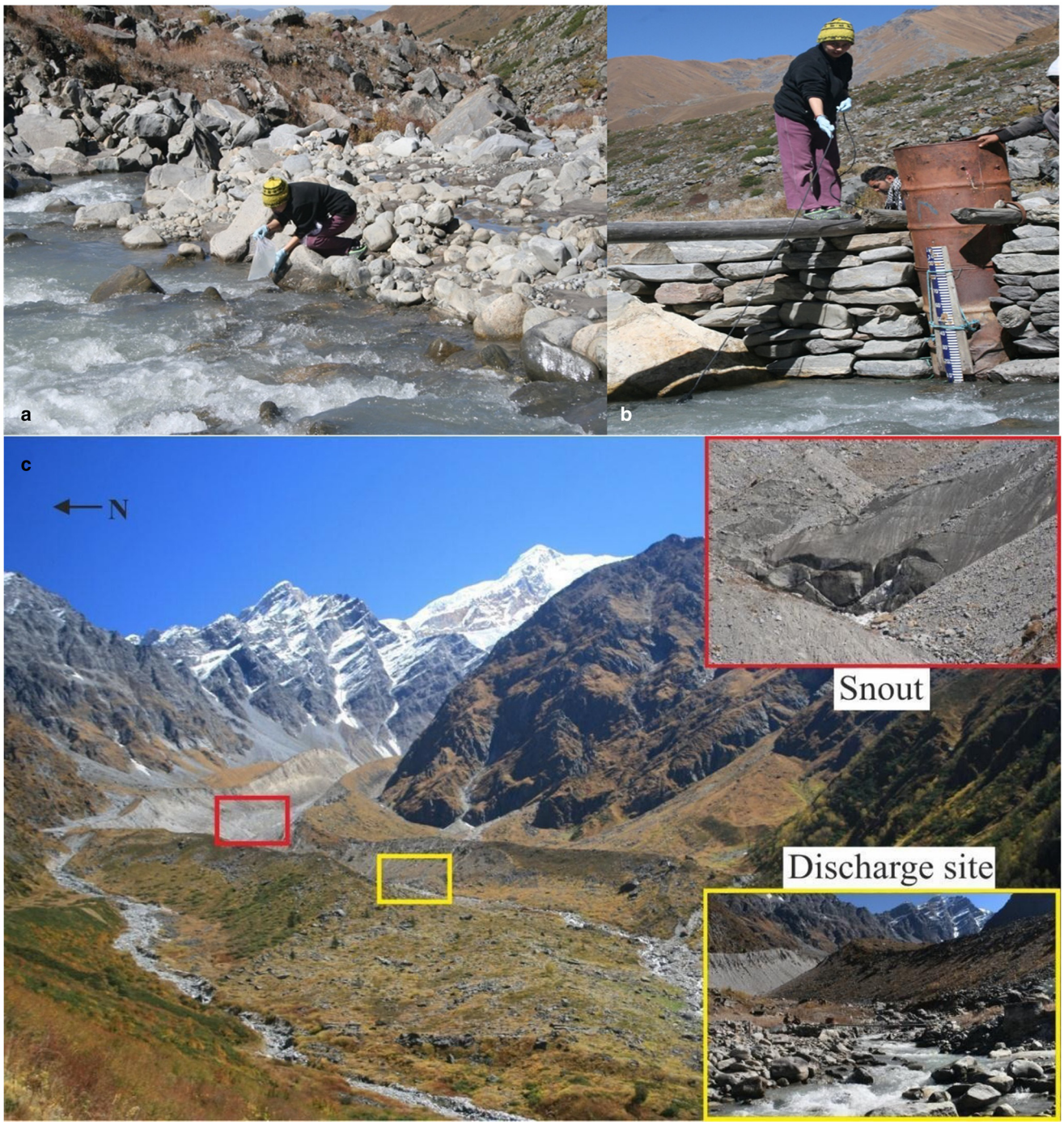

Figure 2. Field photographs showing sampling location and glacier zones of the Dokriani glacier basin. (a, b) meltwater sampling and in situ measurements of physical parameters, (c) glacial snout, discharge site, geomorphological setting like moraine, cliff, etc.

3.3 Analytical calculations

3.3.1 Precipitation corrections

As the site is more prone to the atmospheric transport of moisture from the ocean, therefore, we applied atmospheric input corrections to major ionic concentrations. The ionic concentration corrected for atmospheric input has been denoted with a '*' mark. Corrections were based on the principal quotients between major ion concentration and Cl^- from snowpit are as following: $SO_4^{-2}/Cl^- = 1.47$, $Na^+/Cl^- = 0.42$, $K^+/Cl^- = 0.019$, $Ca^{2+}/Cl^- = 2.86$, $Mg^{2+}/Cl^- = 0.27$ (Sundriyal and others, 2018). Here Cl^- was considered as a conservative ion for correction due to its atmospheric origin. The presence of Cl^- in terrestrial rocks of the catchment is not yet reported. Also the contribution of additional Cl^- through Himalayan cold and warm springs could also be neglected as we found low Cl^- concentration and negative saturation index with respect to halite that suggest the input of Cl^- from springs are negligible here. All other corrections of solute concentrations were done as follows.

$$^{*}X = {}^{\text{total}}X - {}^{\text{total}}Cl^- (X/Cl^-)_{\text{snowpit}}$$

where, *X = concentration of corrected solute concentration
$^{\text{total}}X$ = total concentration of ion
$^{\text{total}}Cl^-$ = total concentration of Cl^- ion in the sample
(X/Cl^-) = snowpit ratio of ion X:Cl^- in snowpit

3.3.2 Cation and fraction of cation contributions from silicate and carbonate weathering

Since the cations Na^+, K^+, Ca^{2+} and Mg^{2+} were derived from silicate mineral bearing rocks and Ca^{2+}, and Mg^{2+} were derived from

https://doi.org/10.1017/jog.2023.108 Published online by Cambridge University Press

carbonate weathering. Major ions values in μeL^{-1} were used for calculations. Therefore, we used the following relationships to explain the river chemistries:

Silicate weathering calculations

$$Na_{sil}^{+\,total} = Na_{riv}^{+\,*}$$
$$K_{sil}^{+\,total} = K_{riv}^{+\,*}$$
$$Ca_{sil}^{2+\,total} = Na_{sil}^{+\,total} \times (Ca^{2+}/Na^{+})_{sil}$$
$$Mg_{sil}^{2+\,total} = Na_{sil}^{+\,total} \times (Mg^{2+}/Na^{+})_{sil}$$

Carbonate weathering calculations

$$Ca_{carb}^{2+\ total} = Ca_{riv}^{2+} * - Ca_{sil}^{2+\,total}$$
$$Mg_{carb}^{total} = Mg_{riv}^{2+} * - Mg_{sil}^{2+\,total}$$

where the superscript $(Ca^{2+}/Na^{+})_{sil}$ and $(Mg^{2+}/Na^{+})_{sil}$ ratios represents the their respective ratios in silicate rocks in the drainage basin. We used the values 0.7 ± 0.3 and 0.3 ± 0.2 for $(Ca^{2+}/Na^{+})_{sil}$ and $(Mg^{2+}/Na^{+})_{sil}$ respectively (Krishnaswami and Singh, 1998).

3.3.3 Sulfate mass fraction

Further, the sulfate mass fraction (SMF) was measured to explain the dominance of sulfide oxidation to carbonate dissolution reactions. An SMF equal to 0.5 shows the predominance of sulfide oxidation reaction coupled to carbonate dissolution. When the SMF is < 0.5, carbonate carbonation reaction dominates. An excess of SMF > 0.5 suggests additional sources of sulfate originating from the Sulfide Oxidation coupled to the silicate weathering reaction, carbonate precipitation or Ca and Mg efflorescent salt dissolution (Cooper and others, 2002; Tranter and others, 2002). SMF is calculated by the following equation:

$$SMF =^{*} SO_4^{-2}/(SO_4^{2-} + HCO_3^{-})$$

where, $^{*}SO_4^{2-}$ = concentration of sulfate, corrected for atmospheric input ($\mu Eq\ L^{-1}$)

HCO_3^{-} = concentration of bicarbonate ($\mu Eq\ L^{-1}$)

3.3.4 PHREEQC model

PHREEQC modeling was used to calculate the saturation indices and the tendency for dissolution/precipitation of minerals and the partial pressure of CO_2 (pCO_2). We used the PHREEQC software using the MINTEQ database (Parkhurst and Appelo, 2013). The concentration of dissolved constituents (Ca^{2+}, Mg^{2+}, Na^{+}, K^{+}, SO_4^{2-}, HCO_3^{-} and Cl^{-}), water temperature and pH were used as data input. Model results are presented in supplementary table S6. The equivalent fractions of the major cation (Ca^{2+}, Mg^{2+}, Na^{+}, K^{+}) and anion (SO_4^{2-}, Cl^{-}, NO_3^{-}) data are reported in supplementary table S6.

All the datasets generated from analytical calculations are presented in supplementary tables S7 and S8.

3.3.5 Cencentration-discharge (c-Q) relationship

The c-Q relationships are widely used technique to trace hydrochemical processes that controls the runoff chemistry (Godsey and others, 2009). These are linear logarithmic plots representing a power-law relationship between concentration and discharge where the slope has physical relationship. We used a power law function (i.e. $\log(c) - \log(Q)$) to describe the relationship by using following equation:

$$c = aQ^{b}$$

here 'c' represents the ionic concentration of stream water in question and 'Q' represents discharge. Further, 'a' is the intercept in units of concentration, and 'b' is a unitless exponent representing the slope of the log-transformed c-Q relationship. We used daily mean concentration of ions available with corresponding discharge as input data. We classified c-Q relationships for transport limited with slopes greater than 0.2, source limited as slope less than −0.2 and datasets behaving chemostatically as −0.2 and 0.2. We used Pearson's 'r' to assess the strength of each annual concentration discharge relationship calculated above. Annual c-Q slopes were classified as statistically significant based on the critical value with an α value of 0.1 and $n - 2$ degrees of freedom based on the number of days included in the annual regression. Pearson's r provides a metric for determining when there is no, low or high correlation between concentration and discharge reflected in the c-Q slope.

4. Results and discussion

The present dataset has allowed us to examine the overall dominance of chemical weathering type and its effect over ionic release from the proglacial stream of meltwater emerging from Dokriani glacier basin. We explored below the origin and source of atmospheric inputs, ionic chemistry for early, peak and late ablation seasons in light of lithology, climate and discharge controls. The variability of ionic release presented here increase our understandings for specific chemical reactions that controls the ionic release at Himalayan glacial basins.

4.1 Chemical characteristics of precipitation and supraglacial waters

To better understand the chemistry of the proglacial stream emerging from the snout of Dokriani glacier basin, we first examined the precipitation chemistry as snowfall, rainfall and supraglacial waters. It represents deposition of atmospheric pollutants and suspended dust particles in the snow. The deposition chemistry was assessed using snow samples collected through snowpit profiling. We reassessed the ionic variability of two snowpit profiles collected at an altitude of 4350 and 4364 m a.s.l. during the study period of 2013–2015 (Sundriyal and others, 2018). The observed K^{+}/Na^{+} (0.42), Mg^{2+}/Na^{+} (0.27) and Ca^{2+}/Na^{+} (3.66) ratios in the snowpit samples were significantly higher than sea salts ratios i.e. K^{+}/Na^{+} (0.02), Mg^{2+}/Na^{+} (0.11) and Ca^{2+}/Na^{+} (0.02). This suggests that the ionic contribution from terrestrial sources is higher than atmospheric deposition at Dokriani glacier basin. However, the concentration of SO_4^{2-} ion was similar to Ca^{2+} which could be correlated with the dissolution of carbonate dust in supraglacial melt waters during melting (Tranter and others, 2002; Stachnik and others, 2016). Earlier observations also support the fact that the contribution of Na^{+}, K^{+}, Ca^{2+} and Mg^{2+} is principally controlled by various other factors like weathering, and industrial or biological missions (Nijampurkar and others, 1993; Singh and Ramanathan, 2017; Singh and others, 2020). Furthermore, it was also observed that the ratio between the different ions like Cl^{-}/Na^{+}, K^{+}/Na^{+}, Mg^{2+} /Na^{+} and Ca^{2+}/Na^{+} are elevated in the snow pit compared with those in surface snow. It was likely to be explained by the elution effect of snow melting during the peak ablation season. Generally, most of the ions are concentrated on the surface and most of the

https://doi.org/10.1017/jog.2023.108 Published online by Cambridge University Press

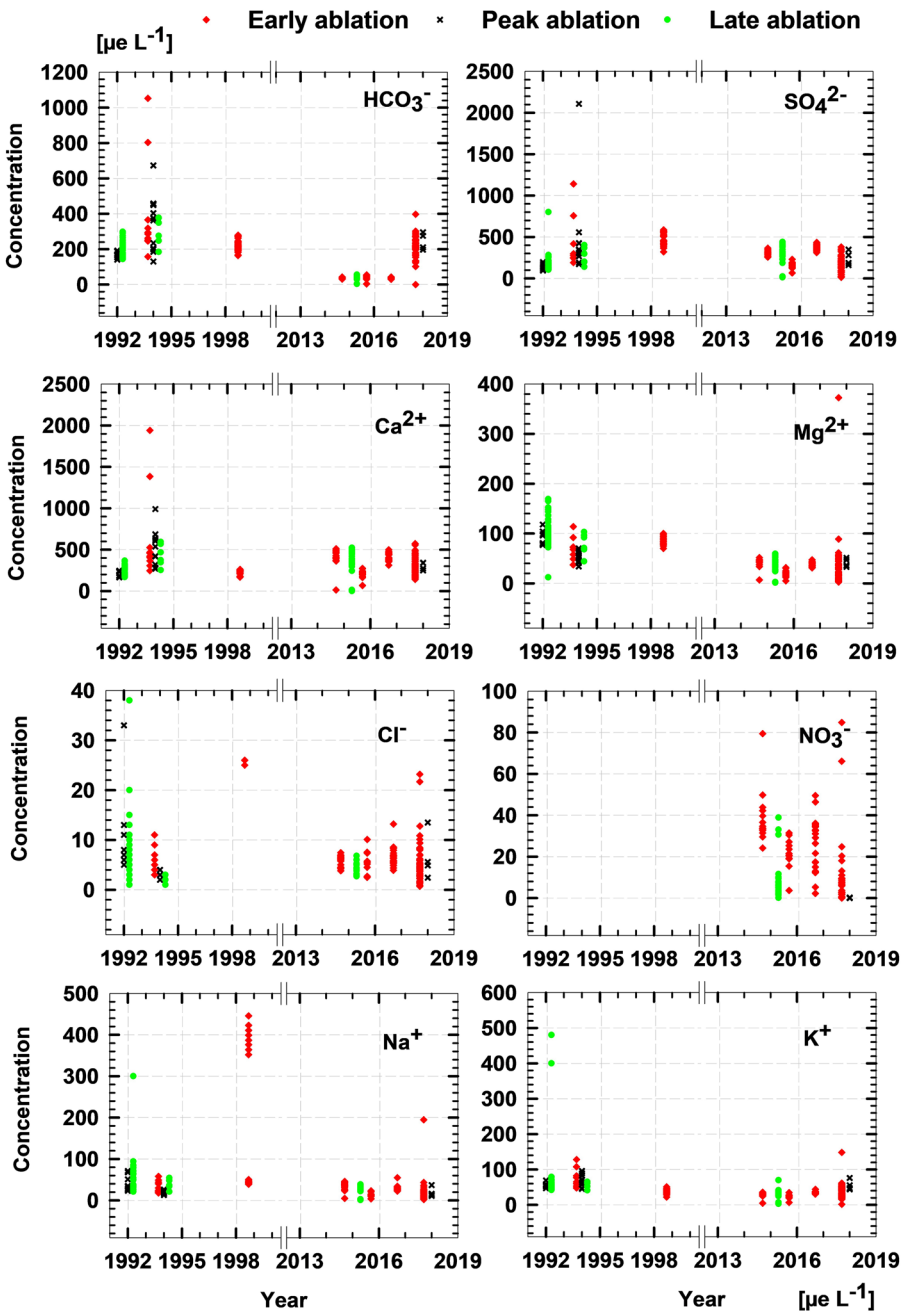

Figure 3. Seasonal concentration of ions representing different ablation at Dokriani Glacier basin. Datasets represent the studies done in years 1992, 1994 (taken from Hasnain and Thayyen, 1996, 1999 respectively); and years 2015 (taken from Tiwari and others, 2018). Rest datasets were generated in the present study. Datasets are presented in supplementary tables S7 and S8.

salts concentrate on the snow surface which easily gets eluted by percolating meltwater. Further, the chemical trends of wet deposition were assessed through ionic concentration of rainfall samples which suggest the variability of major anions ($HCO_3^- > SO_4^{2-} > NO_3^- > Cl^- > F^-$) and cation ($Ca^{2+} > Na^+ > Mg^{2+} > K^+$) follow the similar trends as stream chemistries of the region. Here the HCO_3^- and Ca^{2+} was found to be the most abundant anion and cation in the rainfall respectively.

4.2 Temporal trends of water chemistry at the hydrometric station

To better understand the seasonal variation and quantify the prominent change in the meltwater chemistry at the Dokriani glacier basin, different ablation periods i.e. early ablation, peak ablation and late ablation were studied (Fig. 3). The variabilities observed are presented below:

4.2.1 Early ablation season

Early ablation chemistries of Dokriani glacier basin were first accessed through piper plots (Fig. 4). The results suggest a shift in ionic chemistries, for example, early ablation datasets show that the chemistries of the years 1994 changed from Ca-Mg-HCO_3 type to Ca-Mg-Cl-SO_4 type. We observed the dominance of alkali metals ($Na^+ + K^+$) and HCO_3^- composition in the meltwater during the years 1992 and 1994 respectively. However during the years 2015–2018, alkaline earths metals ($Ca^{2+} + Mg^{2+}$) and SO_4^{2-} were dominant. The early ablation chemistries of years 2015–2018 suggests that the physical parameters recorded from the hydrological site range as follows: pH 5.3 to 7.4, EC from 43.8 to 170 µS cm^{-1}, whereas Na^+ and Cl^- show the range 3.8–54.70 and 2.5–13.2 µE L^{-1} respectively, and SO_4^{2-} shows the highest concentration among anions i.e. from 66.1–433.69 µE L^{-1}. Examined order of variability for ions was as follows: $SO_4^{2-} > NO_3^- > HCO_3^- > F^- > Cl^-$ for anion

https://doi.org/10.1017/jog.2023.108 Published online by Cambridge University Press

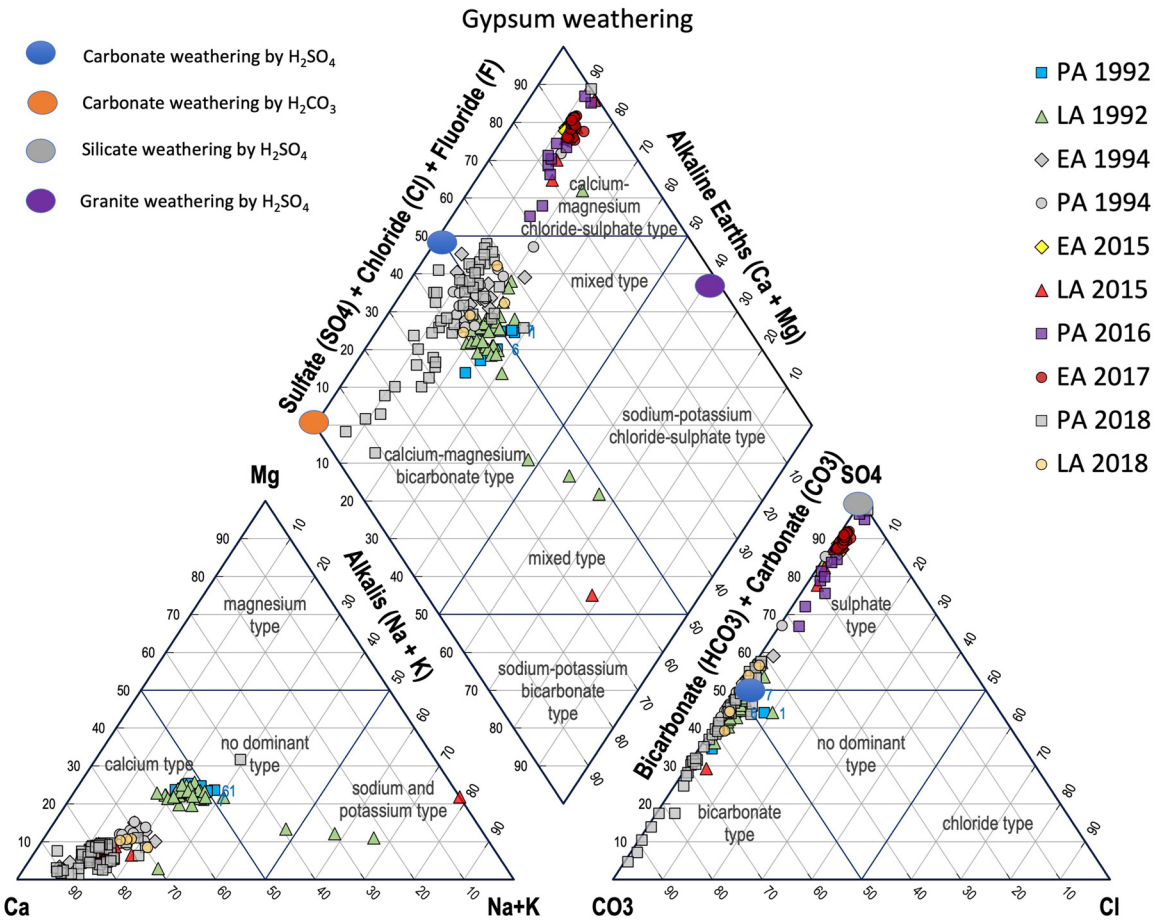

Figure 4. Piper plot of the water samples collected for different ablation seasons between the years 1992 and 2018. For data sources please read Fig. 3 caption. Color symbols reflect the water type and study period. The main rock types by carbonic and sulfuric acid were taken from Spence and Telmer (2005).

and $Ca^{2+} > Mg^{2+} > Na^{+} > K^{+}$ for cation during the early ablation season. The pH value (<7) of the early ablation period suggests a slightly acidic nature of the meltwater stream; however, with in the range of other central and western Himalayan glaciers (Hasnain and Thayyen, 1999; Singh and Ramanathan, 2017). The average concentration and std dev. of the datasets are presented in supplementary table S7. Among the major anions, SO_4^{2-} constitutes up to 80% of TZ^{-} (total anions) concentration and Ca^{2+} a major cation adds up to 76% of TZ^{+} (total cations) concentration. At the start of June month, the concentrations of ions decreased slightly, much likely due to the dilution effect caused by heavy rainfall events. While as the year progressed a slight change (drop) in concentrations for all ions was observed throughout the ablation season. This might be linked with the dilution effect of discharge, however, due to the absence of daily discharge data it is difficult to link with variability of chemical weathering patterns.

4.2.2 Peak ablation season

Similar to early ablation trends, the dominance of alkali metals ($Na^{+} + K^{+}$) and HCO_3^{-} during the years 1992 and 1994 and earth metals ($Ca^{2+} + Mg^{2+}$), and SO_4^{2-} concentrations were observed during the years 2015–2018. This variability was consistent for peak ablation periods as well. The trends of ionic compositions between years 2015 and 2018 at the peak ablation season period were as follows: $SO_4^{2-} > NO_3^{-} > HCO_3^{-} > Cl^{-} > F^{-}$ for anion and $Ca^{2+} > Mg^{+2} > Na^{+} > K^{+}$ for cation. It is much likely that changes in ions compositions were caused due to the leaching of ions from snowmelt. A marked decrease in the ionic concentration was observed during this period that could be correlated with the dilution effect due to excessive rainfall during peak ablation period. The variability observed for the physical parameters and ions are as follows: pH 4.9 to 6.9, EC from 16.3 to 72.4 µS cm^{-1}. The average concentrations value of Na^{+} and Cl^{-} varied between 2.6–194.6 and 0.7–123.1 µE L^{-1} respectively. Similarly, Ca^{2+}, HCO_3^{-} and SO_4^{2-} concentration ranging from 140.8–572.7, 2.1–43.4 and 11.8–379.9 µE L^{-1} during the year 2018.

4.2.3 Late ablation season

The trends of late ablation periods are similar to early and late ablation periods, however we observed that during the years 2015–2018, the shift of alkaline earth metals to bicarbonate become more prominent. The meltwater samples for the late ablation period were collected for the year 2015 during October month. A marked characteristic during this period is identified with the decreased melting rate of the glacier compared to peak ablation period. Subsequently, the ionic concentration has shown increased concentrations particularly for crustal derived elements except the NO_3^{-} and Cl^{-} which is assumed to be derived from the atmosphere (Hodson and others, 2000). The concentration of SO_4^{2-} and Ca^{2+} ion during this season ranges between 311.5–427.4 and 313–508.9 µE L^{-1} respectively for the year 2015. The contribution of SO_4^{2-} ion compared to total anion was upto 40% higher and remained high for the rest of the ablation season. Since the range of variability was higher and in order to assess the overall seasonal

https://doi.org/10.1017/jog.2023.108 Published online by Cambridge University Press

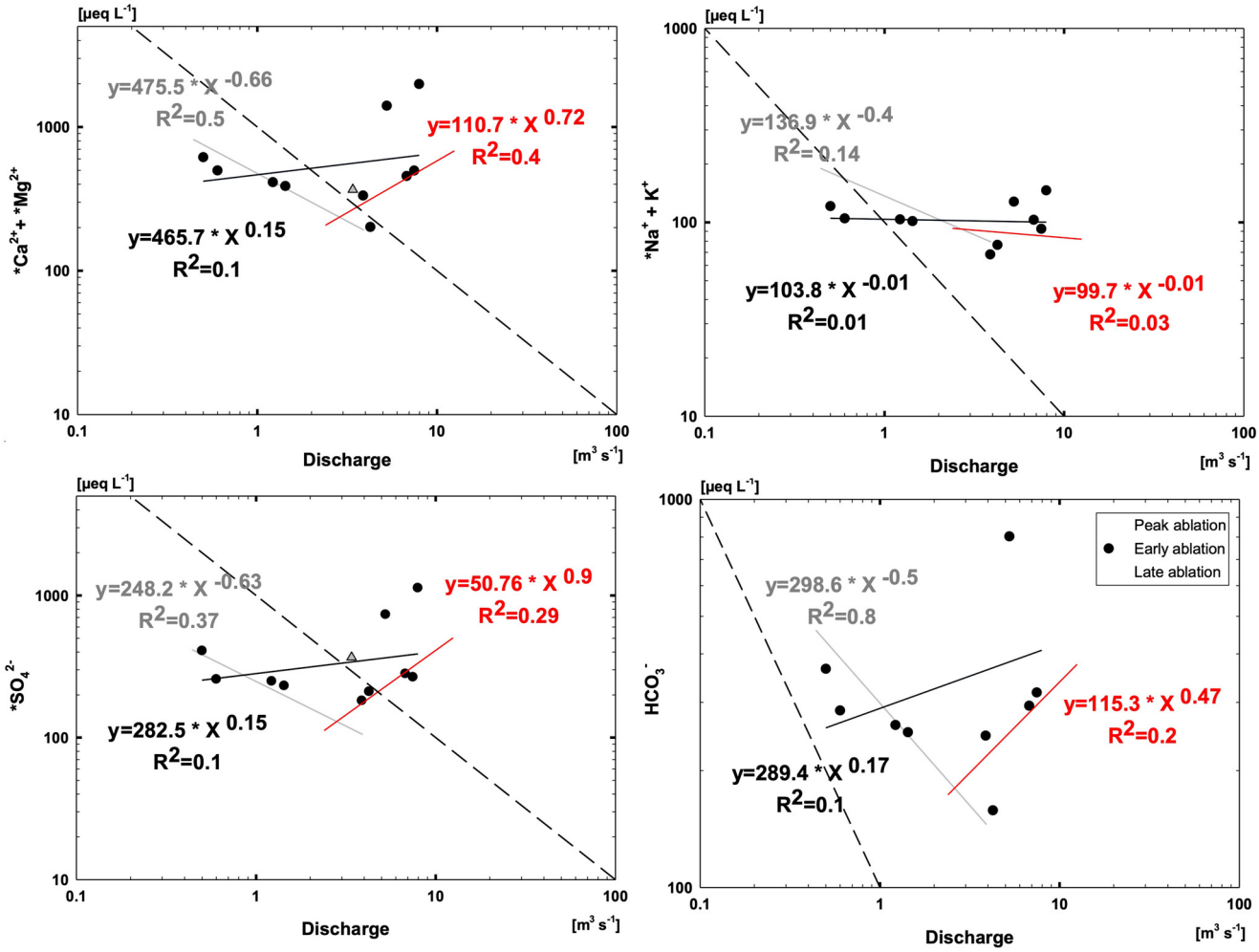

Figure 5. Concentration of conservative ions plotted against discharge variability during different ablation periods at Dokriani glacier basin. Datapoints having corresponding discharge values are presented here between the years 1994 and 2018. Solutes with negative slopes refer to dilution and will have their lowest concentrations at high flows, and thus will exhibit increasing concentrations during hydrograph recession. Because this concentration increase is usually less than proportional to the decrease in discharge, power-law cQ slopes are rarely steeper than −1. Solutes with slopes near zero refer as chemostatic which do not vary systematically with discharge. Solutes with positive slopes refer mobilization which exhibit higher concentrations at high flows, and decreasing concentrations during hydrograph recession. Power-law slopes steeper than 1 indicate that concentrations change more than proportionally to discharge.

ionic stoichiometry and dominance of weathering reactions releasing major ions in meltwater, we used the biplots of dominant cations. Fig. S1 shows a strong correlation of Ca^{2+} and Mg^{2+} ions against total cationic release both for silicate and carbonate weathering. However, the Ca^{2+}, Mg^{2+} release from carbonate minerals lies near the equiline suggest its dominance in meltwater compared to silicate mineral weathering. Figure 3 suggests the trends of ions release from the Dokriani glacier basin have not changed significantly in recent years. However, with bulk chemistry, only speculation could be made regarding the dominance of the chemical weathering type.

The overall trends of meltwater chemistries observed from Dokriani glacier basin suggest that the glacier meltwater has become more acidic over time. This change in the composition of the glacier meltwater over time can be attributed to a number of factors i.e. changing climatic conditions, change in mass balance trends which effects the glacier melt rates, enhance pollutants deposition and successive melting and a few other factors. However, here this could be suggested that these changes indicate contributions from leaching of rocks and soil to meltwater as well. This is true for glacier basins globally therefore the Himalaya is no longer an exception (Nowak and Hodson, 2014; Singh and Ramanathan, 2017; Singh and Kumar, 2022). This could be surmised through the temporal variability presented above that the role of climate or lithology has some control over release of ions from the proglacial stream of Dokriani glacier basin. We explored different possibilities below for control of discharge over ionic release in light of variations in lithology and climate. This allowed us to explain the reaction rates of different minerals that can influence their relative importance in weathering budgets through years along with principal geochemical reactions which originated those ions from the glacier.

4.3 Influence of discharge over ionic chemistries over time: c-Q relationships

To assess the c-Q relationships of major ions released from the glacier basin, all the datasets collected in present study and from published estimates from Dokriani glacier basin have been combined (Fig. 5). This was done as the datasets in the present study is collected for different ablation periods and accurately represents the characteristics of different seasons from Dokriani glacier system. We observed that the c-Q relationships for early, peak and late ablation periods were significantly distinctive (Fig. 5). The early to peak ablation period has witnessed an increase in the average discharge from 2.5 to 5 $m^3 s^{-1}$ much likely

https://doi.org/10.1017/jog.2023.108 Published online by Cambridge University Press

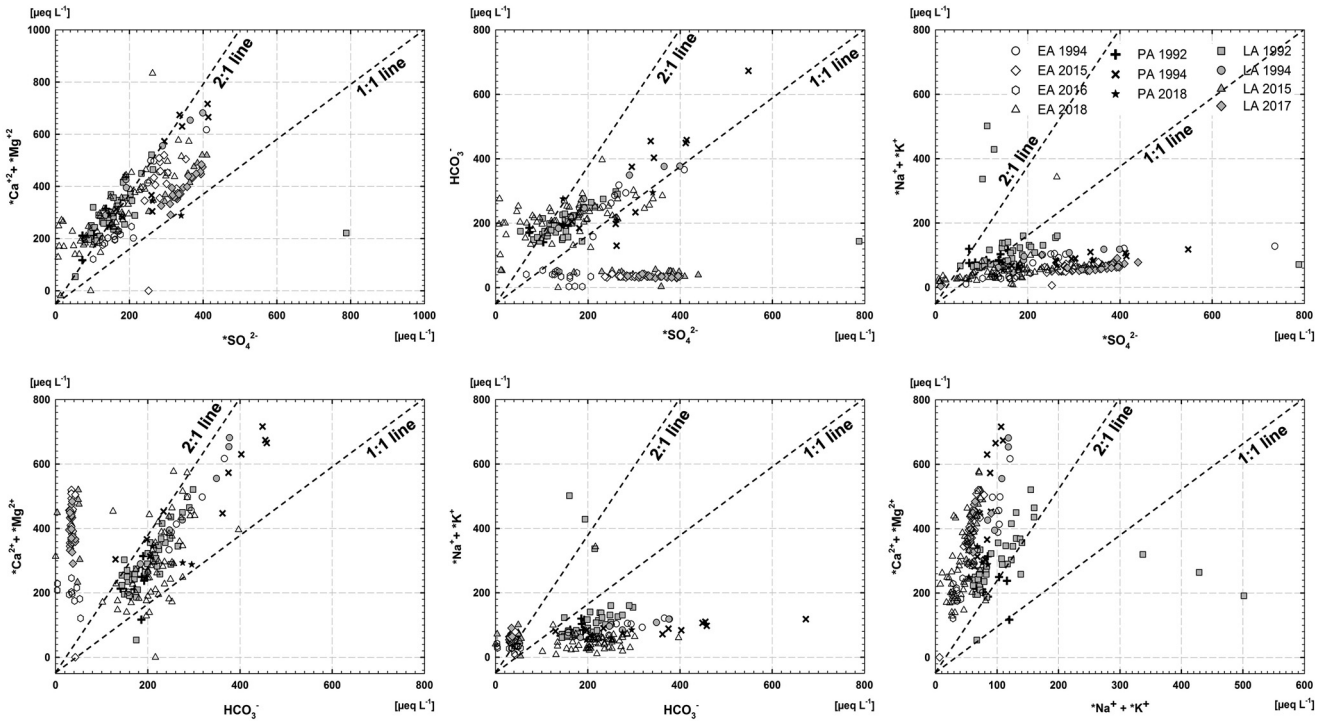

Figure 6. Association of ions for Dokriani Glacier system. Figure present the trends of ionic release resulting from geochemical reactions (Eqns (1)–(7)) operating at the glacial/subglacial system of the Dokriani glacier basin. Data sources are detailed in Fig. 3 caption. Dash lines refer to the release of ions presented in Eqns (1) and (2). For details please refer to section 4.4.

due to increased rainfall and its attendant runoff. This pattern shows a gradual decrease during the late ablation season commencing from the start of late ablation period i.e. September month. Although, the overall trend of c-Q relationship was very weak (>0.2) for all ions, as we observed a decreasing trend initially followed by an increase in discharge values, much likely resulting through the dilution effect. Similarly, we observed some variability for higher discharge values as well particularly for Ca^{2+} ion. For example, correlations for Ca^{2+} ion were observed negative for peak ablation periods, positive for late ablation periods and no significant correlation for early ablation periods. We observed a clear negative slopes of c-Q relationships for peak ablation periods suggesting dilution effect, while a near zero slopes for different early and late ablation periods (e.g. SO_4^{2-}, $Ca^{2+} + Mg^{2+}$ and $Na^+ + K^+$) suggest the system might behave similar to chemostatic behavior of ions. We clarify that the chemostatic behavior of ions should theoretically falls under the slope of −0.2 to 0.2, and except for $Na^+ + K^+$ none fall under this criterion. However, we observed that the trends of peak ablation period datasets are not as identical as early and late ablation periods. For example, the trends of $Ca^{+2} + Mg^{2+}$ with discharge during early and late ablation periods suggest the concentration of ions has increased with respect to discharge. However, during early ablation periods this rate (increasing) was slower compared to the late ablation period. This is much likely due to the slower melting rates during the late ablation period. However, during peak ablation concentration of $Ca^{2+} + Mg^{2+}$ ions first decreased as discharge increases and then we observed a increasing trend, however, the rates were faster than the early and late ablation periods. We explain this variability with higher discharge generated through high rainfall and subsequent fast glacier melting during the peak ablation period. The trends of other ions i.e. $Na^+ + K^+$, SO_4^{2-} and HCO_3^- with discharge has almost followed the trend similar to $Ca^{2+} + Mg^{2+}$ with discharge. Overall, we conclude that the ionic release during early and late ablation periods was controlled by the geochemical reactions operating in the glacial/subglacial zones while the discharge has little or second order effect. While during peak ablation periods we could not be able to draw any conclusions due to a large variability observed in the datapoints.

4.4 Lithological controls of chemical weathering trends in glacial environment

Lithological controls over ionic release were characterized by the availability of H^+ ion that interacted with rock/mineral surface and results in reactions presented below. The reactions (Eqns (1)–(7)) suggests the possible origin of ions in meltwater could through following reactions i.e. dissolution of silicate and carbonate minerals, organic carbon oxidation, sulfide oxidation reaction coupled with carbonate (SOCD)/feldspar dissolution (SOSW) and carbonation of carbonate. The reactions presented here have disproportionate effects on the ionic release and results in a variable change in ionic ratios and compositions. We presented the stoichiometry of ions through scatter plot and linear regressions (Figs 6–8) generated through the reactions listed below, but in different proportions. For example, the SOCD reaction (Eqn (1)) generates the SO_4^{2-} ion at 1 : 2 ratio with HCO_3^- and $Ca^{2+} + Mg^{2+}$, therefore the gradients (as dash lines at Figs 6–8) were presented as a reflection of its stoichiometry. Similarly, the carbonation of carbonates (Eqn (3)) and carbonation of feldspars reaction (Eqn (4)) has slope coefficient of 1 for $Ca^{2+} + Mg^{2+}$ vs HCO_3^- respectively. Plots of HCO_3^- vs SO_4^{2-} in Figure 6 suggests the gradients of ~1 and 2 and also in $Ca^{2+} + Mg^{2+}$ vs SO_4^{2-} reflects the coupling of SOCD reaction via oxic or anoxic mechanism (Tranter and others, 2002; Wadham and others, 2010a; 2010b). Further, the gradients of <1 in HCO_3^- vs SO_4^{2-} ionic plot suggests the process of H^+ generation during oxidation of sulfide minerals that might be used in dissolution reactions of silicate and carbonate minerals occurring simultaneously. Since the Dokriani Glacier is a well-developed valley system with well-defined subglacial drainage networks, gradients of 1 and 2 are close to the predictive frameworks. We noticed that a very low and intermediate gradients of HCO_3^-

https://doi.org/10.1017/jog.2023.108 Published online by Cambridge University Press

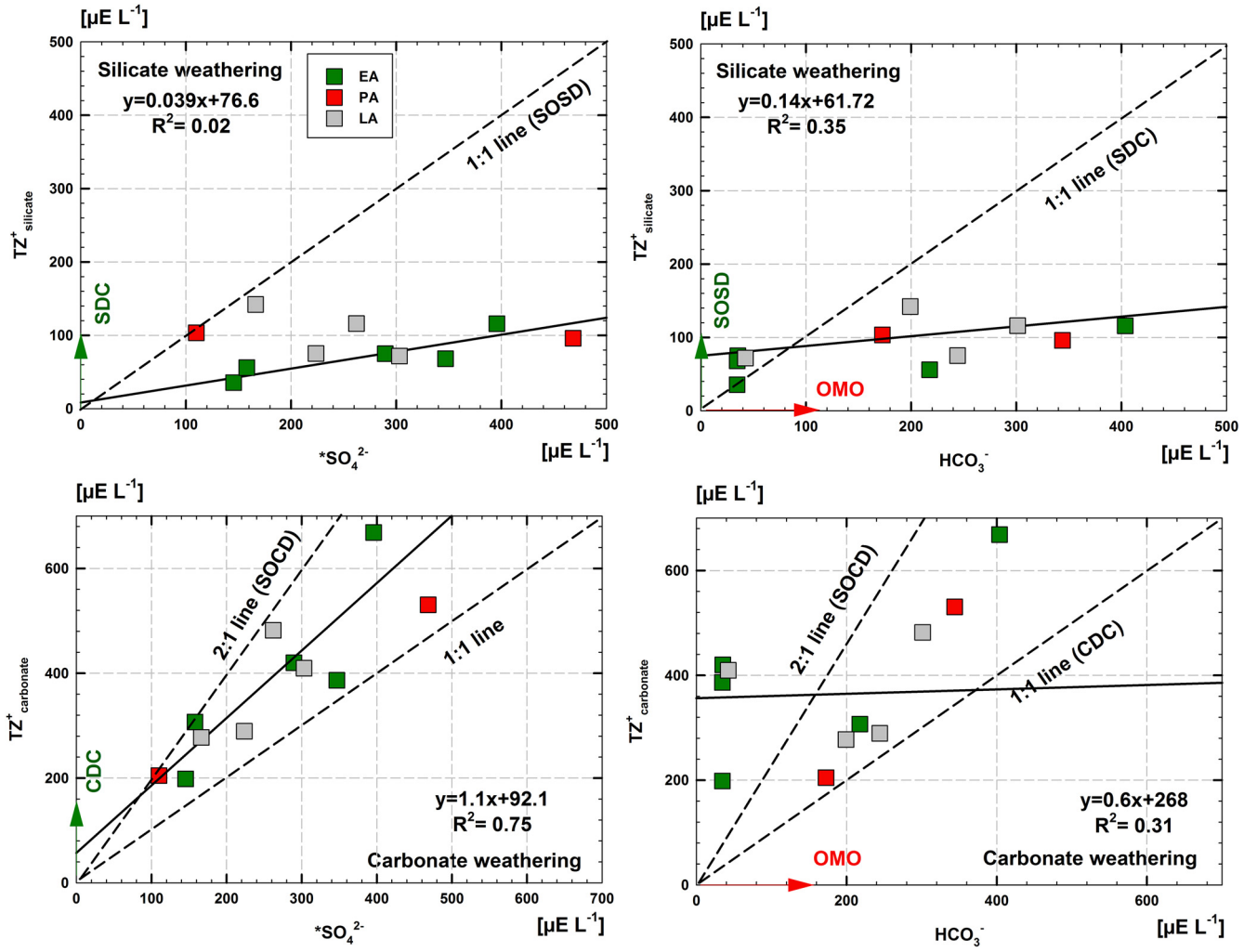

Figure 7. Plots of total cations TZ^+ vs sulfate and bicarbonate ion concentrations for seasonal evolution of ions from Dokriani glacier basin. Here '*' symbol symbolizes the ions corrected for precipitation inputs. The solid line represents orthogonal regression lines for each ablation season with the theoretical slopes (dashed and red arrows). These lines were based on ideal reactions shown in the main text. Data sources are detailed in Fig. 3 caption.

vs SO_4^{2-} in the late ablation periods, which reflect the rapid flushing of ions as surface melt inputs were mostly absent during late ablation periods.

Sulfide oxidation coupled to carbonate dissolution (SOCD)

$$4FeS_2 + 16Ca(Mg)CO_3 + 15O_2 + 14H_2O \rightarrow 16Ca^{2+} + 16Mg^{2+} + 16HCO_3^- + 8SO_4^{2-} + 4Fe(OH)_3 \quad (1)$$

Sulfide oxidation coupled to silicate weathering (SOSW)

$$4FeS_2 + 16NaKAlSi_3O_8 + 15O_2 + 86H_2O \rightarrow 16Na^+ + 16K^+ + 8SO_4^{2-} + 4Al_4Si_4O_{10}(OH)_8 + 32H_4SiO_4 + 4Fe(OH)_3 \quad (2)$$

Carbonation of carbonate

$$Ca(Mg)CO_3 + CO_2 + H_2O \rightarrow Ca^{2+} + Mg^{2+} + 2HCO_3^- \quad (3)$$

Carbonation of feldspar (albite/microcline-orthoclase)

$$2(Na, K)AlSi_2O_8 + 2CO_2 + 9H_2O \rightarrow 2(Na^+, K^+) + 2HCO_3^- + Al_2Si_2O_5 + 4H_4SiO_4 \quad (4)$$

Dissolution of gypsum (an example of efflorescent salts)

$$CaSO_4.2H_2O \rightarrow Ca^{2+} + SO_4^{2-} + 2H_2O \quad (5)$$

Simple hydrolysis of carbonate

$$Ca(Mg)CO_3 + H_2O \rightarrow Ca^{2+} + H_2O \rightarrow H^+ + HCO_3^- \quad (6)$$

Oxidation of organic carbon

$$C_{org} + O_2 + H_2O \rightarrow CO_2 + H_2O \rightarrow H^+ + HCO_3^- \quad (7)$$

Further, Figs 7 and 8 assess the dominance of SOCD reaction in ionic release for different ablation periods and compare with other Himalayan glaciers. The gradient represents products of chemical reactions explained above. The SOCD reaction has slope coefficients of 2.0 to 1.0 for ion associations with total cations (TZ^+) vs SO_4^{2-} and TZ^+ vs HCO_3^- respectively (Eqns (3) and (4)) (Tranter and others, 2002; Wadham and others, 2010a). We noticed that the sulfuric mineral weathering (most probably SOSW, Eqn (2)) is not occurring in concurrence with silicate weathering as all the data sets falling between organic matter oxidation and SDC line in 1 : 1 equliline proportions for the whole ablation season (both in Figs 7 and 8). SOSD reaction

https://doi.org/10.1017/jog.2023.108 Published online by Cambridge University Press

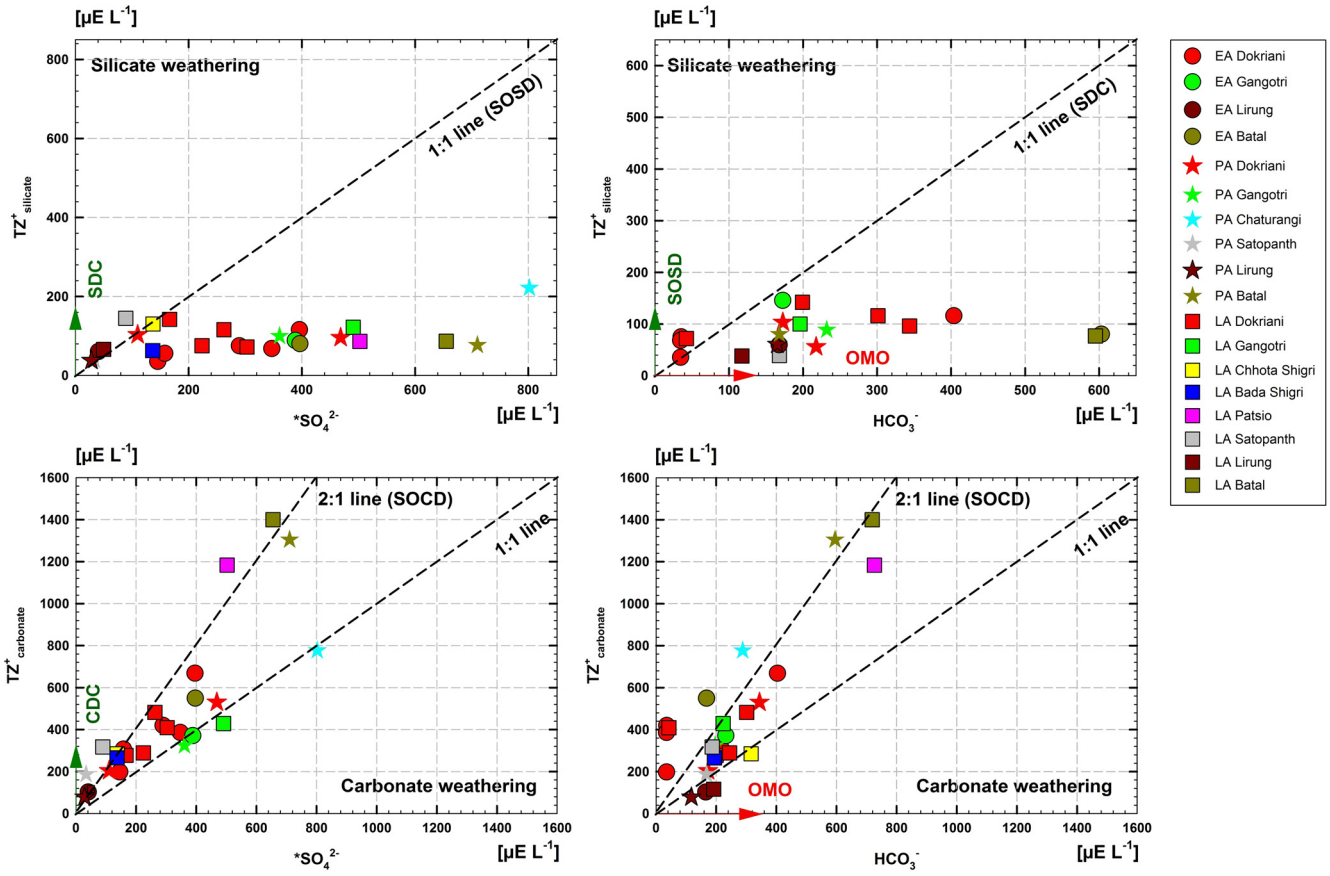

Figure 8. Plots of total cations TZ^+ vs sulfate and bicarbonate ion concentrations from different glacier system of the Himalaya. Here '*' symbol symbolizes the ions corrected for precipitation inputs. The solid line represents orthogonal regression lines for each ablation season with the theoretical slopes (dashed and red arrows). These lines were based on ideal reactions shown in the main text. Data sources are detailed in Fig. 3 caption.

results in the increase of SO_4^{2-} concentrations leading to rise the slope of TZ^+ vs SO_4^{2-} and fall in the slope of TZ^+ vs HCO_3^-. Tranter and others (2002) suggested that this intercept predicts the initial stage of weathering when water comes in contact with rock for the very first time in early ablation seasons and release one Ca^{+2} and HCO_3^- ion in meltwater through the simple hydrolysis reaction (Eqn (6)). However, the higher intercept indicates the production of supplementary H^+ ions formed by other reactions such as the oxidation of organic carbon present in glacial substrate soils (Eqn (7)). In the case of simple hydrolysis through weathering silicate minerals, pH increases but the intercept didn't change. Further, the assumption that if Ca^{+2} and Mg^{2+} was derived mainly from the carbonate weathering then the proportions of SO_4^{2-} and HCO_3^- (Figs 7 and 8) release in meltwater indicates that weathering reactions of sulpate bearing mineral are operational in the meltwater. A decent slope of intercept between TZ^+ vs SO_4^{2-} and TZ^+ vs HCO_3^- ($r^2 = 0.75$ and $r^2 = 0.31$) in Figure 7 confirms that the sulfuric acid mediated reaction has occurred prominently in the subglacial environments of the Dokriani glacier basin. The bivariate plots of total cations (Ca+ Mg + Na + K) at *y*-axis plotted against most domination anions of SO_4^{-2} and HCO_3^- represent the products of carbonate, silicate and sulfuric mineral dissolution process. The observations presented for seasonal variability at Dokriani glacier basin (Fig. 7) shows that the cation release in meltwater is weakly correlated with the SOSD and silicate dissolution through the carbonic acid process. Therefore, the SOSD and SDC mineral weathering effect in the ionic release is very less likely. Further, in bottom two figures (in Fig. 7) suggests the total cationic release from carbonate weathering reactions are dominant and a clear control of SOCD reaction in ionic release in the subglacial reactions is visible. Seasonal effects (mainly discharge) do not seem to have a significant effect on SOCD reaction. Yet some Ca^{2+} and Mg^{2+} ions have been originating along with HCO_3^- which reflects the possibility of simple hydrolysis reaction occurrence in the meltwater drainage from Himalayan glaciers. The results obtained by the seasonal ionic evolution at Dokriani glacier basin are consistent with other Himalayan glaciers as well (Fig. 8).

Overall it has been observed in the Himalayan glaciers that Ca^{2+} and Mg^{2+} is the dominant anion and HCO_3^- and SO_4^{-2} has been the dominant cation in the glacier systems. The trends of seasonal ions release from the Dokriani glacier basin (Fig. 7) and other parts of the Himalaya (Fig. 8) implies that among geochemical reactions listed in Eqns (1)–(7), two reactions i.e. SOCD and carbonate mineral dissolution dominates. The oxidation of FeS_2 could be a key reaction in the subglacial environment having active role in chemical weathering. We observed that the seasonal pattern of ionic release from Dokriani Glacier (Fig. 7) is similar through years i.e. no such change in the reaction patters form 1992 to 2018. Only change we observed in piper plot that the water become more acidic through time. We surmise that since the glacier has retreated significantly (approximately 1 kilometer) in last 28 years and left more fresh mineral surface to react. The high ratio of silicate weathering also explains the presence of active layer on the top of the mineral surfaces which consists of the loose mineral surface, the majority of data suggests that the carbonate phases leached out after that only silicate mineral remain to chemically weather. The nature of weathering reactions observed here indicates the dominance of Ca^{2+}, SO_4^{2-} and HCO_3^- ions in the meltwater chemistries, along with SOCD reaction therefore, the control of specific minerals in lithology over ionic release is evidenced. Therefore, we contend that the bedrock

https://doi.org/10.1017/jog.2023.108 Published online by Cambridge University Press

lithology has a second-order effect over ionic release. The first order control is the chemical weathering reaction typess which operates in the glacial substrats. This assertion could be verified by the fact that Himalayan glaciers are composed of silicate rocks yet the carbonate weathering is dominant. This is true for other glaciers and ice sheets as well and it is much likely due to the rapid kinetics of the carbonate mineral dissolution process worldwide.

4.5 Climatic control over chemical weathering trends

Dokriani glacier basin is an ideal landscape to isolate the effects of climate-induced changes in glacier and chemical weathering trends because it has been studied on long-term basis using field methods and modeling aspects. We used the recent study (Azam and Srivastava, 2020) integrating the field-validated modeling efforts of climate trends and change in the glacial state of Dokriani glacier basin to compare the long-term (1980–2020) chemical weathering trends of the Dokriani Glacier. Our results from the ionic chemistries at the Dokriani glacier basin (Fig. 3) suggest no significant change in concentrations, ionic dominance saturation indices of calcite, pCO_2 levels and SMF fractions (Fig. S2). This could be correlated to near steady-state conditions of the Dokriani glacier between 1992 and 1997 and moderate mass wasting rates between 2007 and 2018 (Azam and Srivastava, 2020). The reason behind more acidic nature of the glacier suggested by the piper plot (Fig. 4), could be correlated to increased mass wasting rates of the Dokriani glacier basin. Corroborated to present study, the increased chemical weathering rates are also observed in previous studies (Li and others, 2022 and references therein). Authors suggested the cation denudation rates has increased upto three times in last two decades. Having positive correlation with temperature, chemical weathering rates are supposed to get higher through time (Li and others, 2022). Yet the overall glacier-wide mass balance was negative in the last four decades, there are no significant changes were observed in mass balance and discharge trends (Fig. S3). Moving further, we applied change point analysis (by using the Past software version 4.11), to detect changes in time series events. The results detect no change in annual, summer mass balance, ELA and AAR yet we observed a distinct trend in a few datasets as winter mass balance has decreased slightly after 2000, however, a slight gain in summer mass balance and discharge is observed (Fig. S4). This change in mass balance trends and discharge has slight impact over the acidic nature and increased ionic release from the Dokriani glacier basin. However, these assertions so not fully explain the control of climate induced mass wasting rates from glacier in question. We contend that similar to lithology, climatic impacts also have second or third-order effects over ionic release. The chemical reactions seem to be controlling the ionic release pattern in the Himalayan glacial basins. Yet more studies are required to ascertain this assumption. Our results highlight a fine balance between weathering mechanisms, and underlying processes linked with climate lithology and glacial intrinsic parameters, yet some accurate assessment of the net effects of weathering budgets on atmospheric chemistry is required further.

5. Conclusions

The Dokriani glacier basin contributes to the river flow of the Bhagirathi River, a major tributary of the river Ganga, one of the major river systems of South Asia. The broader geochemical relevance of the study lies in the fact that long-term geochemical assessment of sulfuric acid-mediated reaction and its impact on ionic release through the glacial basins of the Himalaya. Major observations suggest that the ionic release from Dokriani glacier basin were strongly dominance by the SOCD reactions sourced from sulfuric acid mediated weathering reactions. This process acts as a strong buffer for HCO_3^- ion release in meltwater against carbonate and silicate mineral weathering. The results generated from Dokriani glacier basin is tested in other Himalayan glacierized basins and broadly suggests a second-order control of climate over lithology in the ionic release. We surmise that covariation of sulfide, silicate and carbonate weathering intensity coupled with higher sediment supplies might regulate the sequestration and release of CO_2 on millennium to multi-millennium time scales. We expect the results presented here to be broadly applicable to the many orogenic mountain belts of the world as well.

Supplementary material. The supplementary material for this article can be found at https://doi.org/10.1017/jog.2023.108.

Data. All data are available in the supplementary text as tables.

Acknowledgements. Authors are thankful to scientific and field staff of Wadia Institute of Himalayan Geology, Dehradun, India for their help in various field works. National Institute of Hydrology, Roorkee India is thankfully acknowledged for analytical work support to Shipika Sundriyal. Research funding from Department of Science and Technology, India is acknowledged for Women Scientist Scheme to Shipika Sundriyal (Grant No. SR/WOS-AEA-44/2016). Northwest Institute of Eco-environment and Resources, Lanzhou, China are thankfully acknowledged for providing necessary facilities to complete this work.

Authors' contributions. Conceptualization, writing original draft, analytical calculations: T. S., review & editing: S. C. K., D. P. D., Y. Z., R. S., S. S. and data curation and formal analysis: S. S.

References

Anderson SP, Drever JI, Frost CD and Holden P (1997) Chemical weathering in glacial environments. *Geology* **25**(5), 399–402.

Anderson SP, Drever JI, Frost CD and Holden P (2000) Chemical weathering in the foreland of a retreating glacier. *Geochimica et Cosmochimica Acta* **64**, 1173–1189.

Azam MF and Srivastava S (2020) Mass balance and runoff modelling of partially debris-covered Dokriani glacier in monsoon-dominated Himalaya using ERA5 data since 1979. *Journal of Hydrology* **590**, 125–432.

Berner RA and Canfield DE (1989) A new model for atmospheric oxygen over Phanerozoic time. *American Journal of Science* **289**, 333–361.

Cooper RJ, Wadham JL, Tranter M, Hodgkins R and Peters NE (2002) Groundwater hydrochemistry in the active layer of the proglacial zone, Finsterwalderbreen, Svalbard. *Journal of Hydrology* **269**, 208–223.

Dobhal DP, Gergan JT and Thayyen RJ (2008) Mass balance studies of the Dokriani glacier from to, Garhwal Himalaya, India. *Bulletin of Glaciological Research* **25**, 9–17.

Egli PE, Belotti B, Ouvry B, Irving J and Lane SN (2021) Subglacial channels, climate warming, and increasing frequency of Alpine glacier snout collapse. *Geophysical Research Letters* **48**(21), 680.

Ferrario C, Finizio A and Villa S (2017) Legacy and emerging contaminants in meltwater of three Alpine glaciers. *Science of the Total Environment* **574**, 350–357.

Godsey SE, Kirchner JW and Clow DW (2009) Concentration–discharge relationships reflect chemostatic characteristics of US catchments. *Hydrological Processes: An International Journal* **23**(13), 1844–1864.

Guzzella L and 5 others (2016) POP and PAH contamination in the southern slopes of Mt. Everest (Himalaya, Nepal): long-range atmospheric transport, glacier shrinkage, or local impact of tourism. *Science of the Total Environment* **544**, 382–390.

Hasnain SI and Thayyen RJ (1996) Sediment transport and solute variation in meltwaters of Dokriani glacier (Bamak), Garhwal Himalaya. *Geological Society of India* **47**(6), 731–739.

Hasnain SI and Thayyen RJ (1999) Controls on the major-ion chemistry of the Dokriani glacier meltwaters, Ganga basin, Garhwal Himalaya, India. *Journal of Glaciology* **45**, 87–92.

Heim A and Gansser A (1939) Central Himalaya, geological observations of the Swiss expeditions 1936. *Memorias de la Societe Helvetique des Sciences Naturelles* **73**, I–245.

Hodson A, Tranter M and Vatne G (2000) Contemporary rates of chemical denudation and atmospheric CO_2 sequestration in glacier basins: an Arctic perspective. *Earth Surface Processes and Landforms* **25**, 1447–1471.

Krishnaswami S and Singh SK (1998) Silicate and carbonate weathering in the drainage basins of the Ganga-Ghaghara-Indus head waters: contributions to major ion and Sr isotope geochemistry. *Proceedings of the Indian Academy of Sciences – Earth and Planetary Sciences* **107**, 283–291.

Kumar A, Verma A, Dobhal DP, Mehta M and Kesarwani K (2014) Climatic control on extreme sediment transfer from Dokriani glacier during monsoon, Garhwal Himalaya (India). *Journal of Earth System Science* **123**(1), 109–120.

Li X and 14 others (2022) Globally elevated chemical weathering rates beneath glaciers. *Nature Communications* **13**(1), 407.

Mitchell AC and Brown GH (2008) Modeling geochemical and biogeochemical reactions in subglacial environments. *Arctic, Antarctic, and Alpine Research* **40**, 531–547.

Nijampurkar VN, Sarin MM and Rao DK (1993) Chemical composition of snow and ice from Chhota Shigri glacier, central Himalaya. *Journal of Hydrology* **151**, 19–34.

Nowak A and Hodson A (2014) Changes in meltwater chemistry over a 20-year period following a thermal regime switch from polythermal to cold-based glaciation at Austre Brøggerbreen, Svalbard. *Polar Research* **33**(1), 22779.

Parkhurst DL and Appelo CAJ (2013) Description of input and examples for PHREEQC version 3 – a computer program for speciation, batch-reaction, one-dimensional transport, and inverse geochemical calculations. *US Geological Survey Techniques and Methods* **6**, 497.

Pratap B, Dobhal DP, Mehta M and Bhambri R (2015) Influence of debris cover and altitude on glacier surface melting: a case study on Dokriani glacier, central Himalaya, India. *Annals of Glaciology* **56**(70), 9–16.

Raiswell R (1984) Chemical models of solute acquisition in glacial melt waters. *Journal of Glaciology* **30**(104), 49–57.

Sharp M, Tranter M, Brown GH and Skidmore M (1995) Rates of chemical denudation and CO_2 drawdown in a glacier-covered alpine catchment. *Geology* **23**, 61–64.

Shukla T, Sundriyal S, Stachnik L and Mehta M (2018) Carbonate and silicate weathering in glacial environments and its relation to atmospheric CO_2 cycling in the Himalaya. *Annals of Glaciology* **59**(77), 159–170.

Shukla T, Sundriyal S and Sen IS (2020) Contemporary inorganic carbon fluxes from rapidly changing glacierized watersheds of the Himalaya. *Journal of Hydrology* **587**, 124972.

Shukla T, Sen IS and Sundriyal S (2023) Carbon emissions from emerging glacier-fed Himalayan lakes. *Global and Planetary Change* **225**, 104134.

Singh AK and Hasnain SI (2002) Aspects of weathering and solute acquisition processes controlling chemistry of sub-Alpine proglacial streams of Garhwal Himalaya, India. *Hydrological Processes* **16**, 835–849.

Singh VB and Ramanathan AL (2017) Hydrogeochemistry of the Chhota Shigri glacier meltwater, Chandra basin, Himachal Pradesh, India: solute acquisition processes, dissolved load and chemical weathering rates. *Environmental Earth Sciences* **76**(5), 223.

Singh VB and Kumar P (2022) Hydrogeochemical characteristics of meltwater draining from Himalayan glaciers: a critical review. *Arabian Journal of Geosciences* **15**(8), 680.

Singh VB, Keshari AK and Ramanathan AL (2020) Major ion chemistry and atmospheric CO_2 consumption deduced from the Batal glacier, Lahaul–Spiti valley, western Himalaya, India. *Environment, Development and Sustainability* **22**(7), 6585–6603.

Spence J and Telmer K (2005) The role of sulfur in chemical weathering and atmospheric CO_2 fluxes: evidence from major ions, δ13CDIC, and δ34SSO4 in rivers of the Canadian Cordillera. *Geochimica Et Cosmochimica Acta* **69**(23), 5441–5458.

Stachnik Ł and 6 others (2016) Chemical denudation and the role of sulfide oxidation at Werenskioldbreen, Svalbard. *Journal of Hydrology* **538**, 177–193.

Sundriyal S and 5 others (2018) Deposition of atmospheric pollutant and their chemical characterization in snow pit profile at Dokriani glacier, central Himalaya. *Journal of Mountain Science* **15**, 2236–2246.

Sundriyal S, Shukla T, Tripathee L and Dobhal DP (2020) Natural versus anthropogenic influence on trace elemental concentration in precipitation at Dokriani glacier, central Himalaya, India. *Environmental Science and Pollution Research* **27**, 3462–3472.

Tiwari SK and 6 others (2018) Hydrochemistry of meltwater draining from Dokriani glacier during early and late ablation season, west central Himalaya. *Himalayan Geology* **39**, 121–132.

Torres MA, West AJ and Li G (2014) Sulphide oxidation and carbonate dissolution as a source of CO_2 over geological timescales. *Nature* **507**, 346–349.

Tranter M, Brown G, Raiswell R, Sharp M and Gurnell A (1993) A conceptual model of solute acquisition by Alpine glacial meltwaters. *Journal of Glaciology* **39**, 573–581.

Tranter M and 5 others (2002) Geochemical weathering at the bed of Haut glacier d'Arolla, Switzerland – a new model. *Hydrological Processes* **16**, 959–993.

Valdiya KS (1998) *Dynamic Himalaya*. Universities Press, Hyderabad.

Valdiya KS (1999) Rising Himalaya: advent and intensification. *Current Science* **76**, 0514.

Wadham JL, Hodson AJ, Tranter M and Dowdeswell JA (1998) The hydrochemistry of meltwaters draining a polythermal based, high Arctic glacier, south Svalbard. I. The ablation season. *Hydrological Processes* **12**(12), 1825–1849.

Wadham JL, Cooper RJ, Tranter M and Hodgkins R (2001) Enhancement of glacial solute fluxes in the proglacial zone of a polythermal glacier. *Journal of Glaciology* **47**(158), 378–386.

Wadham JL, Bottrell S, Tranter M and Raiswell R (2004) Stable isotope evidence for microbial sulphate reduction at the bed of a polythermal high Arctic glacier. *Earth and Planetary Science Letters* **219**, 341–355.

Wadham JL, Cooper RJ, Tranter M and Bottrell S (2007) Evidence for widespread anoxia in the proglacial zone of an Arctic glacier. *Chemical Geology* **243**, 1–15.

Wadham JL and 6 others (2010a) Hydro-biogeochemical coupling beneath a large polythermal Arctic glacier: implications for subice sheet biogeochemistry. *Journal of Geophysical Research: Earth Surface* **115**(F4), F04017.

Wadham JL and 8 others (2010b) Biogeochemical weathering under ice: size matters. *Global Biogeochemical Cycles* **24**(3), GB3025.

West AJ, Bickle MJ, Collins R and Brasington J (2002) Small-catchment perspective on Himalayan weathering fluxes. *Geology* **30**(4), 355–358.

White AF and Brantley SL (2003) The effect of time on the weathering of silicate minerals: why do weathering rates differ in the laboratory and field. *Chemical Geology* **202**(3–4), 479–506.

White AF and 5 others (1999) The effect of temperature on experimental and natural chemical weathering rates of granitoid rocks. *Geochimica et Cosmochimica Acta* **63**, 3277–3291.

Williamson MA and Rimstidt JD (1994) The kinetics and electrochemical rate-determining step of aqueous pyrite oxidation. *Geochimica et Cosmochimica Acta* **24**, 5443–5454.

Yde JC, Knudsen NT, Hasholt B and Mikkelsen AB (2014) Meltwater chemistry and solute export from a Greenland ice sheet catchment, Watson River, west Greenland. *Journal of Hydrology* **519**, 2165–2179.

https://doi.org/10.1017/jog.2023.108 Published online by Cambridge University Press